

Minimal attenuation for tunneling through a molecular wire

M. Magoga and C. Joachim

CEMES, Centre National de la Recherche Scientifique, 29 Rue J. Marvig Boîte Postale 4347, 31055 Toulouse Cedex, France

(Received 4 August 1997)

The electronic transmission coefficient through a finite-length molecular wire decreases exponentially when its length increases for energy chosen in its gap. It is demonstrated that the damping factor in the exponential depends on the full wire electronic structure and not only on the gap width as obtained from a WKB calculation of this factor. The gap remains in controlling the minimum of the damping factor. However, this minimum is far from being reached on known molecular wires. An optimization procedure is proposed to define molecular wires with a very small damping in the tunneling regime. [S0163-1829(98)10403-4]

I. INTRODUCTION

Through a finite series of N cells, each made of a transparent part and a less transparent one, waves propagate with a transmission coefficient $T_N(E)$ equal to unity for discrete resonant energies (frequencies).¹ Elsewhere, $T_N(E)$ decreases when N increases, following the exponential law^{1,2}

$$T_N(E) = T_0(E) e^{-2\gamma(E)N}. \quad (1)$$

$\gamma(E)$ is a damping factor characteristic of the interferences of the propagating wave between successive scattering on the cells. Away from the resonances, in the evanescent regime, a question is whether $\gamma(E)$ is bounded from below preventing the propagation to persist through a large- N series of cell. This applies to a variety of problems since this question is obviously related to the phenomenon of band-structure formation when N increases.¹ This is the case in micro-optics with the search for photonic band-gap systems³ and for layered materials to reach a large $\gamma(E)$ with a minimum layer thickness.⁴ Another case, the background of this paper, is the exponential decrease of the elastic conductance of atomic⁵ and molecular wires^{6,7} in the low-bias voltage regime where their current-voltage characteristic is linear.^{8,9} In the elastic tunnel regime, the conductance of a metal-molecule-metal junction reflects the transparency of the molecule to the electrons coming from the electrodes.⁶ This takes into account the possible dephasing between intramolecular tunnel channels,⁶ but not inelastic effects such as vibrational coupling. In this regime and for E belonging to a given electronic gap, $\gamma(E)$ is often considered to depend only on the gap width.¹⁰ This is supported by tight-binding calculations on specific systems¹¹ and by the WKB approximation $\gamma(E) \propto \chi^{-1}$ (Ref. 12) or $\gamma(E) \propto \sqrt{\chi}$ in another approximation.¹⁰ With respect to Eq. (1), an energy gap of width χ is, as usual, the energy range between two energy bands where $T_N(E) = 0$ when the wire length goes to infinity. Notice that long-range electron transfer through a molecule also shows a characteristic exponential decay of its transfer rate as a function of the molecule length.¹³⁻¹⁵ Much work has been devoted to controlling this decay.¹⁶ However, in a through-bond electron transfer experiment the electron-transfer rate is related to the tunneling rate of an electron in a single-molecule conductance experiment and not directly to the elastic conduc-

tance of a molecule. In the following we restrict ourselves to a single-molecule conductance experiment.

In this paper, the exact analytical expression for $\gamma(E)$ as a function of χ is obtained for tunneling through a tight-binding chain considered as a model for finite-length molecular wires. Starting in Sec. II with a standard transfer-matrix approach using a Löwdin effective Hamiltonian technique, we show in Sec. III that $\gamma(E)$ is bounded from below, i.e., for a given family of chains it is not possible to go below a damping limit in tunneling through those wires. It is further shown in Sec. IV, through analytical examples, that this limit is far from being reached on known chains.

II. EXPONENTIAL LAW

Let us consider an infinite chain made of two semi-infinite parts linked in series by a finite chain of N identical cells, different from the semi-infinite ones (Fig. 1). Each cell is made of two different parts A and B to get a finite χ and there are m states in A and in B . In a mono-electronic approximation, the Hamiltonian of the complete system is written

$$H = \sum_{n=-\infty}^{n=0} h(|\phi_n^L\rangle\langle\phi_{n-1}^L| + |\phi_{n-1}^L\rangle\langle\phi_n^L|) + H_{LC} + \sum_{i=1}^{2N} H_{\alpha(i)} + H_{\alpha(i)\omega_i} + \omega_i|\omega_i\rangle\langle\omega_i| + H_{\omega_i\alpha(i+1)} + H_{CR} + \sum_{n=0}^{+\infty} h(|\phi_n^R\rangle\langle\phi_{n+1}^R| + |\phi_{n+1}^R\rangle\langle\phi_n^R|). \quad (2)$$

For odd i , $\alpha(i) = A$ and $\omega_i = \omega_1$; for even i , $\alpha(i) = B$ and $\omega_i = \omega_2$. H_{LC} and H_{CR} are the coupling Hamiltonians between the finite part and the semi-infinite part of the chain.

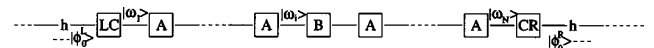


FIG. 1. Tight-binding skeleton of the chain family considered in Eq. (1). Each cell of the finite- N chain is composed of two states $|\omega_i\rangle$ separated by more complex A and B parts with m states per part. This chain is connected left and right through the LC and CR cells to two semi-infinite chains representing the connection pads. Depending on the N parity, the last cell of the finite chain is (or not) integrated in the CR or the LC cell.

The exact matrix elements of $H_{\alpha(i)\omega_i}$, $H_{\omega_i\alpha(i+1)}$, H_{LC} , H_{CR} , H_A , and H_B need not be specified for the demonstration presented here. The only hypothesis on the finite chain is that A and B in a cell are coupled to each other through a single $|\omega_i\rangle$ state only (Fig. 1). There are $2m+2$ states per cell in the finite chain.

An effective, one state per site, chain is readily obtained from Eq. (2) by partitioning the state space of the chain into two parts: one generated by the $|\phi_n^L\rangle$, $|\phi_n^R\rangle$, and $|\omega_i\rangle$ states (projector P) and the other generated by all the $2m \times N$ states of the A and B parts of the cells (projector Q). On the P subspace, the $H|\phi\rangle = E|\phi\rangle$ eigenvalue problem is equivalent to the effective Lowdin eigenvalue problem $H_{\text{eff}}P|\phi\rangle = EP|\phi\rangle$ with the effective Hamiltonian $H_{\text{eff}} = PHP + PHQ(E-H)^{-1}QHP$.^{17,18}

Through a chain containing a single propagative channel, $T_N(E) = |F_{11}(E)|^{-2}$, with $F(E)$ the transfer matrix.¹⁸ $F(E)$ is a nonunitary transformation of the spatial propagator $G(p, -p, E)$ defined from the left to the right part of the chain through the N cells by¹⁹

$$\begin{bmatrix} c_{p+1} \\ c_p \end{bmatrix} = G(p, -p, E) \begin{bmatrix} c_{-p} \\ c_{-(p+1)} \end{bmatrix}, \quad (3)$$

with

$$G(p, -p, E) = K(E)^p A(E) [M_1(E) M_2(E)]^N B(E) K(E)^p$$

and c_i the coefficients of the $P|\phi\rangle$ decomposition on the P subspace. The elementary propagator $K(E)$ is defined through a unit cell of the semi-infinite parts, $A(E)$ and $B(E)$ are the interface propagators from the semi-infinite to the finite parts of the chain, and $[M_1(E) M_2(E)]^N$ is the propagator from one end to the other along the finite chain. The $M_i(E)$ matrices are easily constructed from the H_{eff} matrix elements. The transfer matrix $F(E) = \tilde{A}(E) D(E)^N \tilde{B}(E)$ is obtained after a diagonalization $D(E)$ of the $M_1(E) M_2(E)$ matrix.²⁰ The \tilde{a}_{ij} and \tilde{b}_{ij} matrix elements of $\tilde{A}(E)$ and $\tilde{B}(E)$ accommodate this $M_1(E) M_2(E)$ diagonalization and the $A(E)$ and $B(E)$ nonunitary transformation from the propagator to the transfer matrix. Therefore, $T_N(E)$ is given by

$$T_N(E) = \frac{1}{|\tilde{a}_{11}(E) \tilde{b}_{11}(E) \lambda_+(E)^N + \tilde{a}_{12}(E) \tilde{b}_{21}(E) \lambda_-(E)^N|^2}, \quad (4)$$

with $\lambda_+(E)$ and $\lambda_-(E)$, the two $M_1(E) M_2(E)$ eigenvalues.

For large but finite N and because $\lambda_-(E) = \lambda_+(E)^{-1}$,²⁰ the exponential behavior in Eq. (1) for the tunneling regime is recovered using Eq. (4):

$$T_N(E) = T_0(E) e^{-2N \ln|\lambda_+(E)|}. \quad (5)$$

Compared to equivalent calculations for a series of potential barriers and wells,¹ the improvement in the demonstration of Eq. (1) presented here is that the Hamiltonians H_A and H_B in a cell can be more complex than the one of a potential well. For example, states with different symmetry can be included and the parameters controlling each state in A and B are accessible independently.

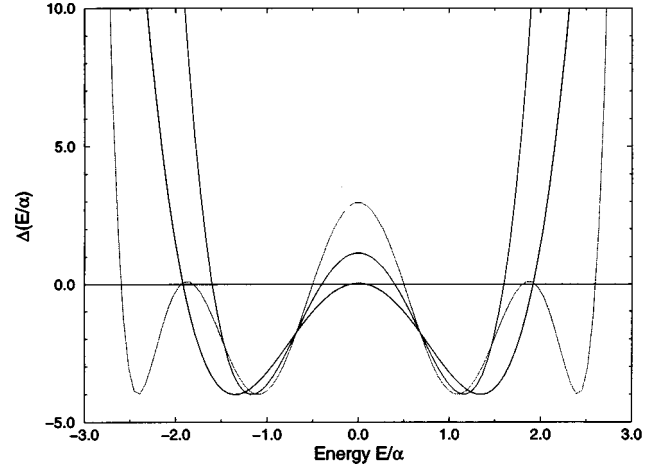


FIG. 2. Examples of the polynomial $\Delta(E)$ calculated for the $d^0[\Delta(E)] = 4$ chain in Fig. 3(a) (---) and is the $d^0[\Delta(E)] = 8$ chain in Fig. 3(c) (—). The parameters chosen are $\alpha'/\alpha = 0.6$, $\alpha/\gamma = 0.1$, $\beta/\delta = 1.0$, and $\beta/\alpha = 3.31$, respectively. -.- is also for the $d^0[\Delta(E)] = 8$ chain in Fig. 3(c), but with the nonoptimized parameters $\alpha/\gamma = 0.91$, $\beta/\delta = 0.93$, and $\beta/\alpha = 1.5$.

III. BOUNDING OF THE DAMPING FACTOR

A simple question is whether or not for a given chain structure $\lambda_+(E)$ can take any value. For example, in the tunneling regime and far from the resonance, it would be interesting to get a $\lambda_+(E)$ as small as possible. The secular equation giving the $\lambda_{\pm}(E)$ roots in Eq. (5) is simply the standard second-order Kramers equation²⁰

$$\lambda(E)^2 - \text{Tr}[M_1(E) M_2(E)] \lambda(E) + \det[M_1(E) M_2(E)] = 0. \quad (6)$$

Since by time-reversal invariance $\det[M_1(E) M_2(E)] = 1$, the two roots of Eq. (6) result in

$$\lambda_{\pm}(E) = \frac{\sqrt{\Delta(E) + 4} \pm \sqrt{\Delta(E)}}{2}, \quad (7)$$

with $\Delta(E) = \text{Tr}[M_1(E) M_2(E)]^2 - 4$.

Obviously, for N going to infinity, the energy intervals where $\Delta(E) \leq 0$ correspond to the location of the electronic bands of the chain and the ones where $\Delta(E) > 0$ to the gaps of this band structure.^{1,21} The zeros of the $\Delta(E)$ polynomial provide the bandwidths and the band gaps of the structure. For a large but finite N , the position of the $\Delta(E)$ zeros control also the damping of the tunneling phenomenon through a finite chain (Fig. 2). However, in the $\Delta(E) > 0$ energy intervals, what happens for a finite N as a function of the intrinsic cell structure surprisingly was not studied in the past. Therefore, answering the question about the minimum possible value of $\gamma(E)$ in Eq. (1) demands from Eqs. (5) and (7) a careful study of the $\Delta(E)$ polynomial, outside the energy range normally of interest for band-structure calculations (Fig. 2).

Taking, for example, an odd number of states in A and B ($m = 2p - 1$), it is easy to show that $d^0[\Delta(E)] = 8p$. In this case, $\Delta(0)$ is the largest positive value of $\Delta(E)$ inside the energy interval containing all the E_i 's $\Delta(E)$ roots. Therefore, the study of $\gamma(E)$ can be restricted to $E = 0$ because in this case $\gamma(0) = \ln[\lambda_+(0)]$ and $\gamma(0)$ is the largest damping factor

inside this interval. From Eq. (7) and using the factorization $\Delta(E) = \prod_{i=1}^{4p} (E - E_i)(E + E_i)$, one obtains

$$\gamma(0) = \ln \left(\frac{\chi \Pi + \sqrt{(\chi \Pi)^2 + 16}}{4} \right). \quad (8)$$

$\chi = 2|E_1|$ is the width of the central band gap of the chain with $|E_1|$ the smallest $\Delta(E)$ root and $\Pi = \prod_{i=2}^{4p} E_i$ is the product of all the other positive roots.

This exact expression does not depend on a specific form of H_A and H_B . It must be opposed to the standard approximations where $\gamma(0)$ is found to depend only on χ .^{10,12} In Eq. (5), all the $\Delta(E)$ roots contribute to determine the damping factor. The consequence of Eq. (8) is the difficulty, for a given χ , to lower Π independently of χ because the coefficients of the polynomial $\Delta(E) = \Delta(0) + a_1 E^2 + \dots + a_{4p-1} E^{2(4p-1)} + E^{8p}$ are all dependent on the same H_{eff} matrix elements. Obviously, the value of a given $\Delta(E)$ root cannot be fixed independently of the others. Due to this rigidity of the $\Delta(E)$ roots, equivalent to the eigenvalue repulsion phenomenon,²² there is a minimization of $\gamma(0)$ by a function of χ . Using the Ostrowski inequality²³ to the $\Delta(E)$ roots, we obtain after some calculations

$$\Delta(0) \geq \frac{\chi^2}{2p} \left(a_2 + \sqrt{a_2^2 - \frac{2pa_1^2}{\chi^2}} \right). \quad (9)$$

However, from Eq. (7), $\lambda_+(0)$ is only a function of $\Delta(0)$. Therefore, $\gamma(0)$ is bounded from below by a function of χ . This is the result obtained, showing that for a given χ it will be difficult to reach a $\gamma(0)$ close to zero since each χ value imposes a limitation on the minimum reachable damping factor. This originates from the Hamiltonian eigenvalue repulsion phenomenon. However, as shown below for a few examples, the best known molecular wires are far from this limit.¹¹ Therefore, the lower limit can be the pivot for a better optimization of the wire structure to reach a very small $\gamma(0)$.

IV. ANALYTICAL EXAMPLES

The simplest chain structure with $\chi \neq 0$ is of the $d^o[\Delta(E)] = 4$ type because with $d^o[\Delta(E)] = 2$ there is only one electronic band with no gap. Two generic chains with $d^o[\Delta(E)] = 4$ are known: the polyene $(\text{CH})_x$ and the poly(sulfonitride) $(\text{SN})_x$ (Ref. 24) whose simple tight-binding representation is recalled in Fig. 3. In this representation, the polynomials can be calculated analytically with $\Delta(E) = y^{-2} E^4 - 2E^2 y^{-1} (y + y^{-1}) + (y - y^{-1})^2$ for $(\text{CH})_N$ and $\Delta(E) = E(E - \bar{a})(E^2 - E\bar{a} - 4)$ for $(\text{SN})_{N/2}$. The dimerization coupling ratio is $y = \alpha' / \alpha$ for $(\text{CH})_N$ (Ref. 11) and \bar{a} is the first ionization potential difference between S and N in this oversimplified model of $(\text{SN})_{N/2}$ (Ref. 24) with, respectively, $\chi = 2(\alpha' - \alpha)$ for $(\text{CH})_N$ and $\chi = \bar{a}$ for $(\text{SN})_{N/2}$. These polynomials are of the form $\Delta(X) = X^4 - 2bX^2 + c$ and their roots can be obtained analytically. This leads to $\lambda_+(0) \geq \sqrt{\chi^4/64} + \sqrt{\chi^4/64 + 1}$, which is a better lower limit than Eq. (9) because it is restricted to a specific $d^o[\Delta(E)] = 4$ family of tight-binding chains.

The lower limit of $\gamma(0)$ as a function of χ defines a forbidden region on the $\gamma(0) - \chi$ chart. This is presented in

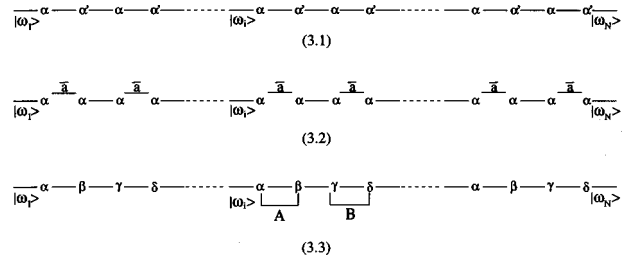


FIG. 3. Tight-binding skeleton of the three finite chains whose $\gamma(0) - \chi$ charts are given in Fig. 4. (a) is a model for the $(\text{CH})_N$ chain, (b) for the $(\text{SN})_{N/2}$ chain, both with $d^o[\Delta(E)] = 4$, and (c) a model for the $d^o[\Delta(E)] = 8$ optimized chain. The α , α' , β , and γ parameters are the coupling matrix elements between the atomic levels used to model the $(\text{CH})_x$ and $(\text{SN})_x$ chains. \bar{a} stands for the first ionization potential difference between S and N in an over simplified model of $(\text{SN})_x$ (Ref. 24).

Fig. 4 together with the $\gamma(0) = f(\chi)$ curves for $(\text{CH})_N$ and $(\text{SN})_{N/2}$, which are easily obtained analytically. These curves develop far from the forbidden region given by the $\Delta(X)$ lower limit because this lower limit was obtained with independent b and c parameters. With a tight-binding chain, b and c are obviously related imposing a constraint on the $\Delta(E)$ roots. To attenuate this constrain and reach the $d^o[\Delta(E)] = 4$ forbidden region in Fig. 4, we have constructed a new family of tight-binding chains. This is a $d^o[\Delta(E)] = 8$ chain with $m = 1$ [Fig. 3(c)]. A complete exploration of its control parameter space was possible because its $\Delta(E)$ roots can still be obtained analytically. This optimization leads to a specific repartition of the tight-binding coupling over the unit cell of the chain with $\alpha/\gamma = 0.1$ and $\beta/\delta = 1.0$. As presented in Fig. 4, for a given χ , $\gamma(0)$ is always much smaller in this case than for a $(\text{CH})_N$ or a $(\text{SN})_{N/2}$ chain. This is a verification that χ is not the only parameter controlling the damping. An interesting aspect of

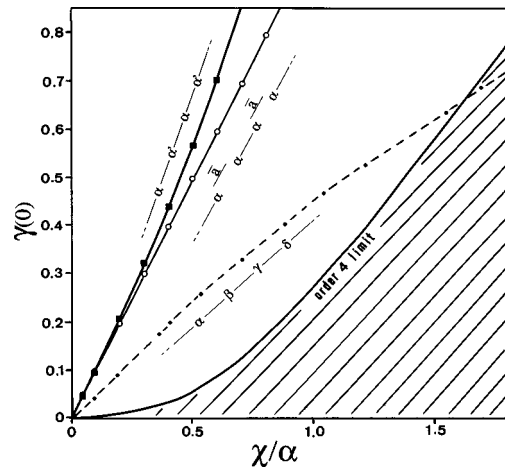


FIG. 4. Variation of $\gamma(0)$ as a function of the gap χ for the $(\text{CH})_N$, $(\text{SN})_{N/2}$, and $d^o[\Delta(E)] = 8$ chains given in Fig. 3. The forbidden region of the $\gamma(0) - \chi$ chart is obtained by the $d^o[\Delta(E)] = 4$ dedicated minoration. The $d^o[\Delta(E)] = 8$ curve is obtained by selecting the best $\lambda(0)$ for a given χ with $\chi = \sqrt{2}(A - \sqrt{A^2 - 4B^2})^{1/2}$, $A = \alpha^2 + \beta^2 + \gamma^2 + \delta^2$, $B = (\delta\beta - \alpha\gamma)$, and then $\lambda(0) = \beta\delta/\alpha\gamma$.

the strategy to increase $d^o[\Delta(E)]$ for a better $\gamma(0)$ is that the optimized $\gamma(0)=f(\chi)$ curve for $d^o[\Delta(E)]=8$ penetrates the $d^o[\Delta(E)]=4$ forbidden region on the $\gamma(0)-\chi$ chart. This means that by a better architecture of each part of the unit cell of the finite chain, $\gamma(0)$ is controllable. The difficulty is to translate in a chemical formula the optimized tight-binding skeleton.

V. CONCLUSION

The damping factor of the transmission coefficient in the tunneling regime is often related only to the electronic gap width of the chain. We have demonstrated how this damp-

ing is controlled by the complete electronic band structure of the chain. Our demonstration was restricted to a particular energy value but can be generalized easily to all gap intervals of an electronic band structure. Families of tight-binding chains have been presented, showing very different damping factors for the same gap. It remains that the gap width is quite influential because it fixes the minimum accessible damping. But this lower limit is still far away from the damping factor of known molecular wires. This opens the way to design molecular wires that will transport current in a tunneling regime in the long range.

We would like to thank the ESPRIT IV Nanowires project for financial support during this work.

-
- ¹C. Cohen-Tannoudji, B. Diu, and F. Laloe, *Mecanique Quantique* (Hermann, Paris, 1977), Vol. I, p. 366.
- ²L. Brillouin and M. Parodi, *Propagation des Ondes dans les Milieux Periodiques* (Masson, Paris, 1956).
- ³T. F. Krauss, R. M. De La Rue, and S. Brand, *Nature* (London) **383**, 699 (1996).
- ⁴C. Boudas, J. V. Davidivits, F. Rondelez, and D. Vuillaume, *Phys. Rev. Lett.* **76**, 4797 (1996).
- ⁵L. Pizzagali, C. Joachim, X. Bouju, and C. Girard, *Europhys. Lett.* **38**, 97 (1997).
- ⁶M. Magoga and C. Joachim, *Phys. Rev. B* **56**, 4722 (1997).
- ⁷V. Mujica, M. Kemp, and M. A. Ratner, *J. Chem. Phys.* **101**, 6856 (1994).
- ⁸C. Joachim and J. K. Gimzewski, *Europhys. Lett.* **30**, 409 (1995).
- ⁹A. Yazdani, D. M. Eigler, and N. Lang, *Science* **272**, 1921 (1996).
- ¹⁰M. Samanta, W. Tian, S. Datta, J. I. Henderson, and C. P. Kubiak, *Phys. Rev. B* **53**, R7626 (1996).
- ¹¹C. Joachim and J. F. Vinuesa, *Europhys. Lett.* **33**, 635 (1996).
- ¹²K. H. Gundlach, *J. Appl. Phys.* **44**, 5005 (1973).
- ¹³H. M. McConnell, *J. Chem. Phys.* **35**, 508 (1961).
- ¹⁴C. Joachim, *Chem. Phys.* **116**, 339 (1987).
- ¹⁵J. W. Evenson and M. Karplus, *J. Chem. Phys.* **96**, 5272 (1992).
- ¹⁶M. D. Newton, *Chem. Rev.* **91**, 767 (1991).
- ¹⁷P. O. Lowdin, *J. Math. Phys.* **3**, 969 (1962).
- ¹⁸C. Joachim and P. Sautet, in *Scanning Tunneling Microscopy and Related Methods*, Applied Science Series E, edited by R. J. Behm, N. Garcia, and H. Rohrer (Kluwer, Dordrecht, 1990), Vol. 184, p. 377.
- ¹⁹J. Stein and C. Joachim, *J. Phys. A* **20**, 2849 (1987).
- ²⁰P. Sautet and C. Joachim, *Phys. Rev. B* **38**, 12 238 (1988).
- ²¹A. H. Wilson, *The Theory of Metals* (Cambridge University Press, New York, 1965).
- ²²T. A. Brody, J. Flores, J. B. French, P. A. Mello, A. Pandey, and S. S. Wong, *Rev. Mod. Phys.* **53**, 385 (1981).
- ²³P. Ostrowski, *J. Math.* **44**, 42 (1965).
- ²⁴J. S. Miller, *Extended Linear Chain Compounds* (Plenum, New York, 1982), Vol. 2.